Studying the Role of ERK Inhibition in Glioblastoma Multiforme

Rumela Mitra, M. Aswanth Harish, and Bithiah Grace Jaganathan

Keywords ERK inhibition · Cancer · Glioblastoma · Sorafenib · BVD523 · BIX02188 · ERK1/22

1 Introduction

Glioblastoma or glioblastoma multiforme (GBM), originating in the glial cells of the brain, is classified by WHO as a grade IV astrocytoma and has an extremely poor prognosis with a 5-year survival rate of 5% after diagnosis [1]. Conventional therapy using temozolomide [2–4] along with radiotherapy or surgery fails to prevent disease relapse, primarily due to the presence of residual cancer stem cells (CSCs) [5]. Constitutive activation of several signaling cascades in CSCs, such as the mitogen-activated protein kinase or MAPK pathway [6, 7], promotes chemoresistance [8], tumor heterogeneity and disease progression [9].

Upregulation of growth factor receptors that belongs to the receptor tyrosine kinase (RTK) family in GBM leads to the downstream activation of the MAPK/ERK pathway [10]. In addition, high phosphorylated ERK levels correlate with higher proliferation and invasion capacity of GBM cells. Inhibition of the MEK/ERK1/2 pathway increases ECM adhesion and reduces the migration ability of the cells [11]. The FDA-approved pan-RTK inhibitor sorafenib is a drug that is orally administered [12] to patients in the advanced stages of hepatocellular carcinoma (HCC) and

R. Mitra · M. Aswanth Harish · B. G. Jaganathan (✉)
Stem Cell and Cancer Biology Research Group, Department of Biosciences and Bioengineering, Indian Institute of Technology Guwahati, Guwahati, Assam, India
e-mail: bithiahgj@iitg.ac.in

B. G. Jaganathan
Jyoti and Bhupat Mehta School of Health Sciences and Technology, Indian Institute of Technology Guwahati, Guwahati, Assam, India

L. M. Pandey et al. (eds.), *Healthcare Research and Related Technologies*,
https://doi.org/10.1007/978-981-99-4056-1_7

renal cell cancer [13]. It inhibits proliferation and angiogenesis in HCC, often used in combination with other therapeutic agents [14–16] and also inhibits the migratory and invasive abilities of breast cancer cells in vitro [17]. Sorafenib targets the cell-surface RTKs (including VEGFR, PDGFR-β, c-KIT and Flt-3) as well as intracellular serine/threonine kinases (like Raf-1 and wild-type or mutated B-RAF) [18, 19]. Ulixertinib (BVD523), a reversible, small molecule inhibitor, has a high selectivity for ERK1/2. BVD523 inhibits the proliferation of cancer cells, upregulates apoptosis-related genes, and attenuates ABCB1 and ABCG2-mediated chemoresistance [20, 21], making it a suitable candidate for treating drug-resistant cancers. Preclinical trials with BVD523, in combination with or without other chemotherapeutic agents, have shown promising outcomes [22–24]. Another ERK inhibitor, BIX02188, targets ERK5 by inhibiting the kinase activity of MEK5 [25]. Although not very well characterized, BIX02188 induces apoptosis in FLT3-mutated cancers such as AML [26].

In the current study, the GBM cell line U87MG was treated with sorafenib, BVD523 and BIX02188 their effect on proliferation, survival, migration and self-renewal was determined. We found that pan-RTK inhibition significantly downregulated the proliferation and migration of glioblastoma cells compared to the selective inhibition of ERK1/2, whereas ERK5 inhibition alone did not produce any significant effect.

2 Materials and Methods

2.1 Differential Gene Expression and Pathway Analysis

The clinical data of glioblastoma patients and their respective mRNA expression profiles were obtained from The Cancer Genome Atlas (TCGA) database (https://cancergenome.nih.gov/). TCGA-Glioblastoma multiforme (GBM) dataset contains 169 GBM samples and five normal samples. R statistical software (version 4.1.3; https://www.r-project.org/) and Bioconductor packages (http://www.bioconductor.org/) were used to process and normalize the raw data. The Limma package was utilized to identify the differential gene expression between the normal and tumor tissues. Pathway enrichment analysis for differentially expressed genes was determined using gProfiler.

2.2 Reagents and Cell Lines

High glucose DMEM, propidium iodide and protease inhibitor cocktail were obtained from Sigma-Aldrich. Fetal bovine serum, trypsin, phosphatase inhibitor cocktail, primary antibodies (anti-human) against phosphoERK1/2, beta-catenin, BCL2,

GAPDH and HRP conjugated secondary antibodies (anti-mouse and anti-rabbit) were procured from ThermoFisher Scientific. Fluorescent dye conjugated antibody against CD24 was purchased from ThermoFisher Scientific. BVD523 and BIX02188 were purchased from Selleck Chemicals LLC. Sorafenib was purchased from Natco Pharma Ltd. Glioblastoma cell line U87MG was purchased from NCCS, Pune, and plastic wares for cell culture were purchased from Eppendorf.

2.3 Colony Assay

Colony assay was carried out as previously described [27]. 100 cells/well were seeded in a 6-well plate and treated with the inhibitors. During pre-treatment, inhibitors were added for the initial 48 h, after which fresh media was added to induce the formation of the colonies. In some cases, treatment was extended until the completion of the experiment. The resulting colonies were counted microscopically after staining them with 0.1% crystal violet solution.

2.4 Protein Isolation and Immunoblotting

Cells were seeded, allowed to attach for 24 h, and treated with sorafenib or BVD523 for 48 h. As described previously, cells were lysed using RIPA buffer at the end of treatment period to collect the total protein [17, 27]. ~25 μg protein was loaded per well in a 10% polyacrylamide gel and transferred to a nitrocellulose membrane through semi-dry blotting. The membrane was incubated with the desired antibodies to detect the protein expression level.

2.5 Wound Healing Migration Assay

A previously published protocol was followed for the wound healing migration assay [17, 27]. 10,000 cells/cm^2 were added to each well of a 12-well plate and incubated until they formed a monolayer, following which they were serum-starved for 12 h. A scratch was made using a micro tip, and media containing the respective inhibitors was added to each well. Microscopic images were taken at regular intervals and analyzed further to determine the migration speed.

2.6 Spheroid Assay

Glioblastoma cells were seeded at a density of 0.5–2 $\times$ 10^4 cells/mL in a low-attachment 96-well plate for the formation of spheroids. The spheroids were imaged periodically, and their area was determined using ImageJ software.

2.7 Proliferation Assay

5000 cells/cm^2 were seeded in each well of a 24-well plate and allowed to attach. Cells were then treated with different concentrations of BVD523 for 48 h. The cells were trypsinized, counted, stained with propidium iodide (PI) and analyzed using a flow cytometer.

2.8 Surface Marker Analysis

Cell surface expression of CD24 was determined using a flow cytometer. Cells were trypsinized and stained with fluorescence conjugated antibody against CD24 for 30 min in the dark at 4˚C and analyzed by flow cytometry.

2.9 Cell Cycle Analysis

A previously published protocol was followed to perform cell cycle analysis [28]. Following treatment with the respective inhibitors, the cells were fixed and permeabilized with 70% ice-cold ethanol, followed by RNase A treatment. DNA was stained using PI and analyzed with a flow cytometer.

2.10 Data Analysis

Images from colony and spheroid formation assays were analyzed using the ImageJ software. The migration of cells in the wound healing assay was analyzed using the TScratch software, and flow cytometric data were analyzed with FCS Express5. Quantification of protein bands in the Western blots was done using the ImageLab software (Bio-Rad) and normalized to GAPDH expression levels.

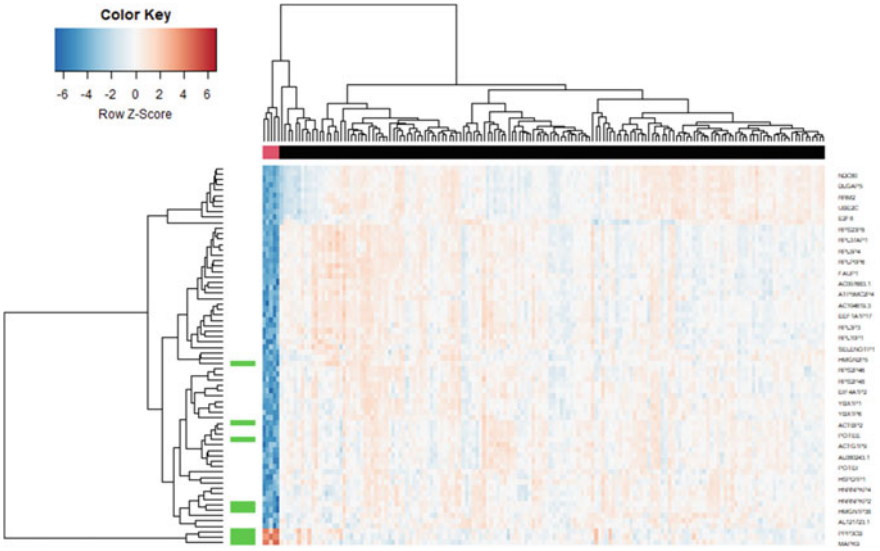

Fig. 1 Heatmap representing differentially expressed genes between normal and glioblastoma patients

3 Results

3.1 Identification of Differentially Expressed Genes and Pathways

The genes that are significantly differentially expressed between normal and glioblastoma tumor samples are shown in the heatmap (Fig. 1). The pathways linked to the differentially expressed genes are shown in the table (Table 1). MAPK signaling pathway was found to be dysregulated in the TCGA-GBM cohorts, along with the Wnt/β-catenin pathway. So, we studied the role of the MAPK pathway in vitro in glioblastoma cells using MAPK pathway inhibitors.

3.2 RTK Inhibition Decreases the Self-renewal, Proliferation and Migration of Glioblastoma Cells

Sorafenib was reported to inhibit the growth of glioblastoma cells and selectively inhibit the tumor-initiating population in primary cells [29, 30]. We previously reported that sorafenib (10 μM) significantly inhibits the proliferative, migratory and invasive abilities of breast cancer cells and modifies their intracellular signaling pathways [17]. Sorafenib treatment inhibited the tumor-initiating ability in GBM, where

Table 1 Pathways associated with differentially expressed genes in glioblastoma indicate dysregulation of the MAPK pathway

Significant	p value	Overlap. size	Term id	Term name
TRUE	0.0179	3	GO:0,002,764	Immune response-regulating signaling pathway
TRUE	0.00689	3	GO:0,002,768	Immune response-regulating cell surface receptor signaling pathway
TRUE	0.00439	2	KEGG:04,659	Th17 cell differentiation
TRUE	0.00851	2	KEGG:04,310	Wnt signaling pathway
TRUE	0.0351	2	KEGG:04,010	MAPK signaling pathway
TRUE	0.00695	2	KEGG:04,728	Dopaminergic synapse
TRUE	0.0138	2	KEGG:05,167	Kaposi sarcoma-associated herpesvirus infection
TRUE	0.0122	2	KEGG:05,152	Tuberculosis
TRUE	0.0178	2	KEGG:05,170	Human immunodeficiency virus 1 infection
TRUE	0.00406	2	KEGG:04,660	T cell receptor signaling pathway
TRUE	0.00623	2	KEGG:04,380	Osteoclast differentiation
TRUE	0.00322	2	KEGG:04,658	Th1 and Th2 cell differentiation
TRUE	0.00431	2	KEGG:04,625	C-type lectin receptor signaling pathway
TRUE	0.0229	2	MIRNA:hsa-miR-1178-3p	hsa-miR-1178-3p

the sorafenib-treated U87MG cells failed to form colonies (Fig. 2a). Furthermore, upon treatment with sorafenib, the GBM cells formed smaller spheroids, indicating that sorafenib inhibits cell proliferation and self-renewal ability (Figs. 2b, 4b). CD24 is a marker of stem cells in several cancers, including glioma [31–34] and we found a significant decrease in the CD24 + population after sorafenib treatment (Fig. 2c–d), suggesting that sorafenib treatment reduces the CSC population in GBM.

Protein expression analysis showed that sorafenib induces the accumulation of phosphoERK1/2 and downregulates the expression of β-CATENIN, implying that cell growth and proliferation were hindered. Further, a reduction in BCL2 expression was observed, which suggests that sorafenib redirected the cells towards apoptosis (Fig. 2e). Thus, we conclude that sorafenib decreases the self-renewal of glioblastoma cells and alters the MAPK/ERK signaling cascade, which is essential for proper cellular functioning.

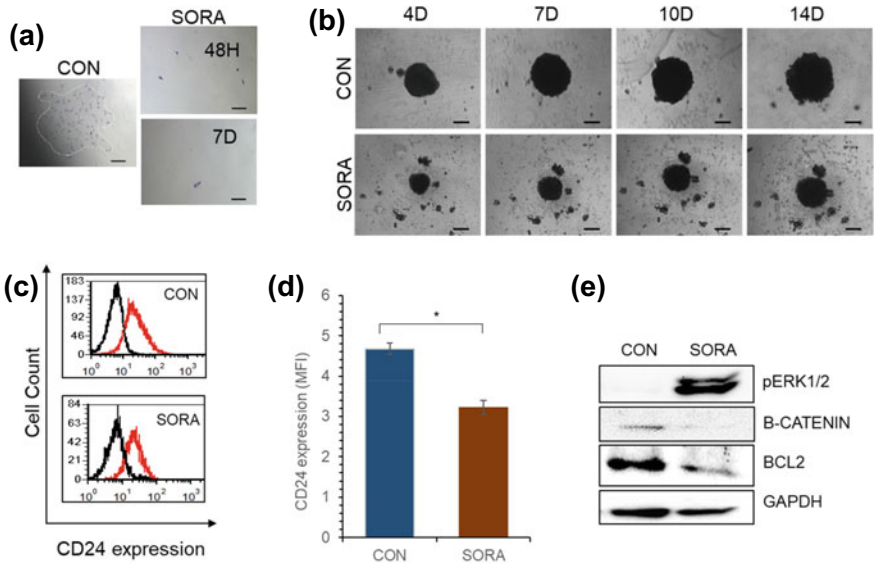

Fig. 2 **a** Colony formation assay was performed with control untreated U87MG cells (CON) or cells treated with sorafenib (SORA, 10 μM) for 48 h (48H) or 7 days (7D) **b** Spheroid formation assay was done without (CON) or with sorafenib treatment, and the spheroids were imaged at the intervals of 4, 7, 10 and 14 days (4, 7, 10, 14D). The black line indicates the scale bar (200 μm) in all the microscopic images **c** Flow cytometry analysis was done to determine the expression levels of CD24 on the surface of U87MG cells in untreated (CON), and sorafenib (SORA) treated cells **d** Represents the normalized Mean Fluorescence Intensity (MFI) of CD24 in U87MG cells. Values are mean ± SE, n = 3, *p < 0.05 **e** Western blotting was performed to determine the expression of phosphorylated ERK1/2 (pERK1/2), BCL2 and β-catenin after 48 h of SORA treatment, CON represents the untreated control cells

3.3 ERK1/2 Inhibition Decreased the Viability of Glioblastoma Cells in a Concentration-Dependent Manner

To further understand the effect of MAPK inhibition in GBM, we treated U87MG with the ERK1/2 selective inhibitor BVD523 (BVD) and determined its effect on proliferation and migration. The viability of U87MG glioblastoma cells decreased with increasing BVD concentration, with an IC_{50} of 10 μM (Fig. 3a, b). This reduction in cell survival was accompanied by a dramatic increase in the accumulation of phosphoERK1/2 and downregulation of β-CATENIN protein levels (Fig. 3c). Based on these results, 10 μM of BVD was used for further experiments.

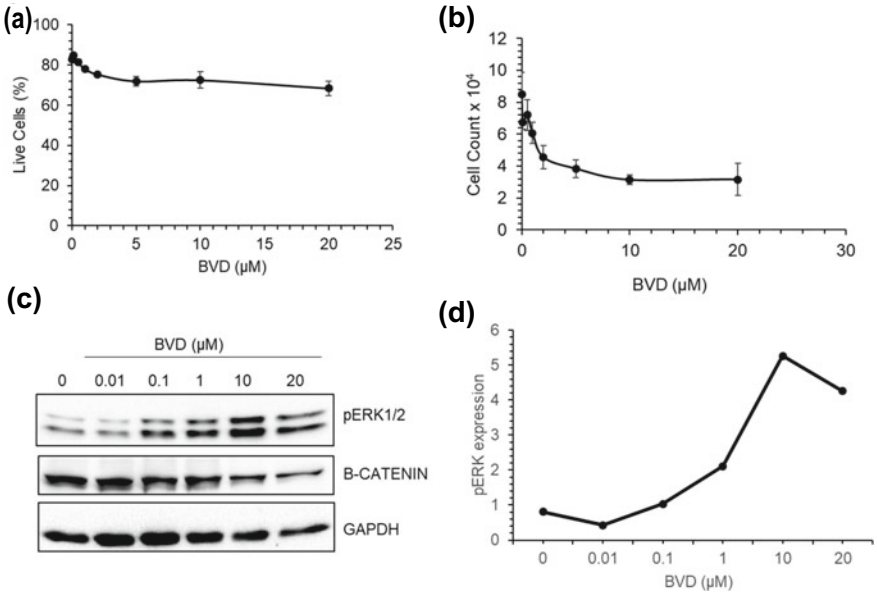

Fig. 3 **a** Live cell percentage post-treatment with the indicated concentrations of BVD523 (BVD) for 48 h was determined by staining with propidium iodide (PI) and analyzed using flow cytometer. **b** The cell count was determined after treatment with BVD for 48 h **c** Immunoblotting analysis was performed to determine the phosphoERK1/2 (pERK1/2) and β-CATENIN expression level after treatment with the indicated concentrations of BVD for 48 h. **d** The pERK1/2 levels shown in **c** were quantified and normalized against their respective GAPDH levels

3.4 ERK1/2 Inhibition Affects the Proliferative, Migratory and Self-renewal Ability of Glioblastoma Cells

Spheroid formation assay was performed to find the effect of BVD on the survival and proliferation of U87MG cells. BVD treatment significantly inhibited spheroid growth, and the inhibitory effect was sustained until 14 days (Fig. 4a, b). Cell cycle analysis showed that BVD treatment induces G0/G1 arrest in U87MG cells (Fig. 4c) in agreement with the reduced proliferation. However, we noticed a significant increase in the expression levels of CD24 after BVD treatment (Fig. 4d, e). BVD treatment, however, lowered the migration ability (Fig. 5a, b) and significantly decreased the colony formation ability (Fig. 5c, d). The colony formation ability was completely abrogated when treatment with BVD was extended beyond 72 h, suggesting that prolonged BVD treatment inhibits the self-renewability of U87MG cells. The effect of BVD on self-renewal was found to be irreversible, where the cells did not regain their colony formation ability when BVD was removed after 72 h of treatment.

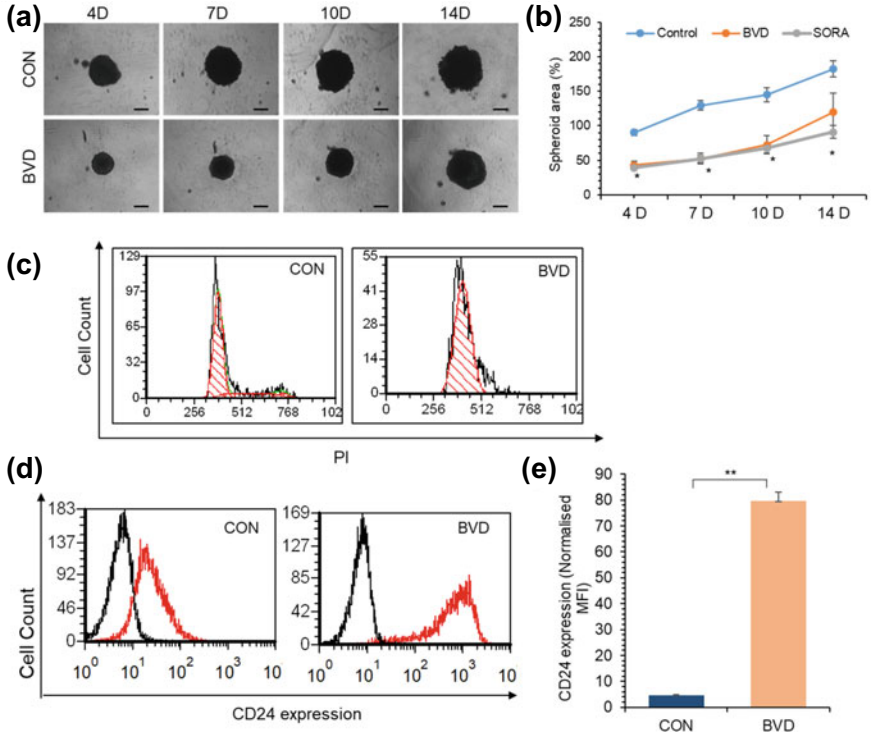

Fig. 4 **a** U87MG cells were allowed to form 3D spheroids in the absence (CON) or presence of BVD523 (10 μM, BVD). The black line shows the scale bar of 200 μm **b** The graph represents the spheroid size of U87MG cells upon treatment with sorafenib (SORA) or BVD523 (BVD) for the indicated time. **c** The cell cycle profile of untreated (CON) and BVD-treated U87MG cells was determined by PI staining through flow cytometric analysis. The histogram shows the cell cycle profile. **d** The cell surface expression of CD24 in control (CON) or BVD (10 μM, 48 h) treated U87MG cells was determined by flow cytometry analysis. The black and red lines indicate the isotype control and CD24 stained sample respectively. **e** Graph represents the CD24 expression levels in control (CON) and BVD-treated U87MG cells. Values are mean ± SE, n = 2–3, $*p < 0.05$, $**p < 0.005$

3.5 *Effect of ERK5 Inhibition on Glioblastoma Migration and Self-renewal Ability*

Next, we studied the effect of MEK5 inhibition on the self-renewal and migration of U87MG cells. MEK5, an upstream activator of ERK5, was inhibited by treatment with BIX02188. MEK5 inhibition did not affect the migration ability of U87MG cells, where the migration speed after treatment with BIX02188 (BIX) was similar to that observed with the control cells (Fig. 5a, b). The migration ability was significantly

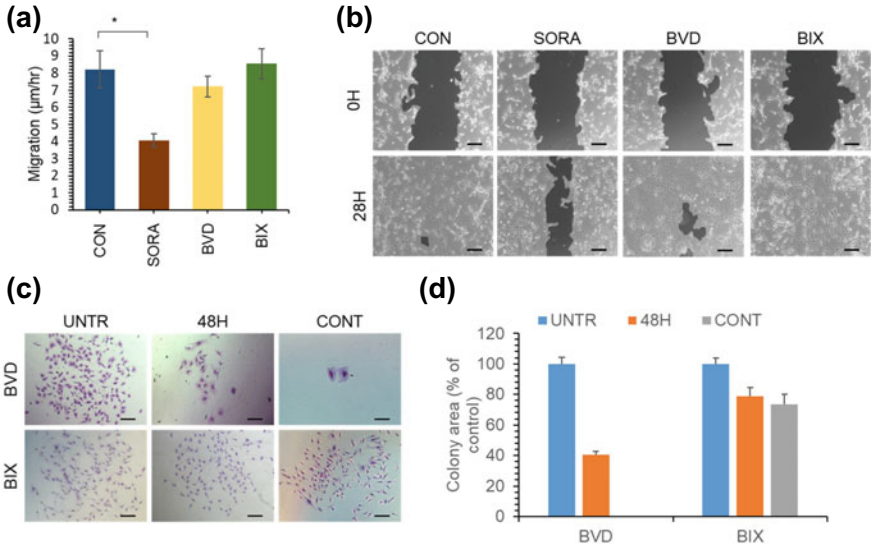

Fig. 5 **a**, **b** Migration of U87MG cells was checked by wound healing assay after treatment with sorafenib (SORA, 10 μM), BVD523 (BVD, 10 μM) and BIX02188 (BIX, 2 μM). **c** The ability of U87MG cells to self-renew was determined by colony formation assay after treatment with BVD or BIX for 48 h (48H) or continuously (CONT) throughout the duration of the assay. UNTR represents the untreated control **d** The graph represents the colony area represented in **c**. Values are mean ± SE, n = 2–3, $*p < 0.05$. The scale bar (200 μm) was indicated by black lines in all the microscopic images

inhibited, however, after sorafenib treatment. Nevertheless, we observed a moderate reduction in the colony formation ability with BIX treatment, and the prolonged treatment with BIX did not further inhibit the ability of U87MG cells to form colonies (Fig. 5c, d).

4 Discussion

Survival of a stem cell-like population in glioblastoma tumors after conventional treatment with temozolomide poses a significant challenge in preventing disease relapse [5]. This highlights the need for alternative therapeutic strategies to target self-renewing and chemoresistant cells in cancer. In this study, we found that MAPK pathway genes were differentially expressed in TCGA-GBM cohorts. So, we initially examined the effects of the broad-spectrum RTK inhibitor sorafenib on the proliferation, migration and self-renewal of glioblastoma cells. As reported by previous studies in glioblastoma [29], breast cancer [17] and hepatocellular carcinoma [35], sorafenib treatment inhibited colony formation in vitro, indicating that sorafenib abrogates the self-renewal ability. This was accompanied by a reduction in the cell

surface expression of CD24, a CSC marker [31–34]. Decreased migration in 2D culture and smaller spheroid size in 3D culture indicate that sorafenib treatment inhibits the metastatic and proliferation ability of glioblastoma cells.

Furthermore, the decreased survival and proliferation ability of GBM cells after sorafenib treatment was indicated by reduced BCL2 and beta-catenin levels, respectively. Interestingly, pERK1/2 levels were upregulated, in contrast to reduced pERK1/2 levels reported in hepatocellular and breast carcinomas [17, 36]. The mechanism of this upregulation in glioblastoma is not well understood but may be caused by the multikinase inhibitory activity of sorafenib on ERK1/2 rather than on its upstream activators, leading to altered feedback loops within the RAS/RAF/ERK pathway.

It is reported that elevated expression of pERK1/2 is associated with glioblastoma progression. In order to understand the mechanism, ERK1/2 inhibitor BVD523 was utilized in this study. BVD effectively reduced cell viability and proliferation in 2D and 3D cultures [37–39] and induced cell cycle arrest. BVD also inhibited the colony formation and migration ability of U87MG cells. BVD treatment altered two intrinsic signaling pathways, the RAS/RAF/ERK pathway and the Wnt/β-catenin pathway. β-catenin downregulation leads to reduced proliferation [40, 41]. However, a concentration-dependent increase of pERK1/2 levels after BVD treatment indicates its aberrant kinase activity rather than its phosphorylation status, thereby preventing activation of downstream targets [20]. Although sorafenib and BVD523 showed a similar effect in terms of abrogating tumor initiation, proliferation and migration, the effects observed were more pronounced with the former, implying that the activity of sorafenib is mediated by ERK1/2 inhibition in conjunction with inhibition of other tyrosine kinase receptors. Selective inhibition of MEK5 kinase activity, thereby ERK5 inhibition with BIX02188, moderately decreased the self-renewal ability of U87MG but did not alter the cell migration. Nevertheless, it cannot be concluded that ERK5 inhibition does not affect tumor proliferation or metastasis since the effect might become pronounced when used in combination with one or more inhibitors.

Thus, sorafenib and BVD523 effectively reduced tumor initiation, proliferation, survival and metastasis by altering the ERK signaling cascade, whereas BIX02188, when used alone, was not effective against the glioblastoma cells. However, combinatorial therapy with drugs and inhibitors that target alternate cellular mechanisms is therapeutically more beneficial than single pathway inhibition.

Acknowledgements RM and AH are supported by a fellowship from the Ministry of Education (MoE), Government of India (GoI). We thank North East Centre for Biological Sciences and Healthcare Engineering (NECBH), IIT Guwahati, for the flow cytometry facility.

References

1. Tamimi AF, Juweid M (2017) Epidemiology and outcome of glioblastoma. In: De Vleeschouwer S (ed) Glioblastoma. Codon Publications Copyright, The Authors, Brisbane (AU)
2. Friedman HS, Kerby T, Calvert H (2000) Temozolomide and treatment of malignant glioma. Clin Cancer Res 6(7):2585–2597
3. Strobel H et al (2019) Temozolomide and other alkylating agents in glioblastoma therapy. Biomedicines 7(3)
4. Zhang J, Stevens MF, Bradshaw TD (2012) Temozolomide: mechanisms of action, repair and resistance. Curr Mol Pharmacol 5(1):102–114
5. Chen J et al (2012) A restricted cell population propagates glioblastoma growth after chemotherapy. Nature 488(7412):522–526
6. Colella B et al (2019) Autophagy induction impairs Wnt/β-catenin signalling through β-catenin relocalisation in glioblastoma cells. Cell Signal 53:357–364
7. Pearson JRD, Regad T (2017) Targeting cellular pathways in glioblastoma multiforme. Signal Transduct Target Ther 2:17040
8. Auffinger B et al (2015) The role of glioma stem cells in chemotherapy resistance and glioblastoma multiforme recurrence. Expert Rev Neurother 15(7):741–752
9. Friedmann-Morvinski D (2014) Glioblastoma heterogeneity and cancer cell plasticity. Crit Rev Oncog 19(5):327–336
10. Guo YJ et al (2020) ERK/MAPK signalling pathway and tumorigenesis. Exp Ther Med 19(3):1997–2007
11. Ramaswamy P, Nanjaiah ND, Borkotokey M (2019) Role of MEK-ERK signaling mediated adhesion of glioma cells to extra-cellular matrix: possible implication on migration and proliferation. Ann Neurosci 26(2):52–56
12. Wilhelm SM et al (2004) BAY 43–9006 exhibits broad spectrum oral antitumor activity and targets the RAF/MEK/ERK pathway and receptor tyrosine kinases involved in tumor progression and angiogenesis. Cancer Res 64(19):7099–7109
13. Bæk Møller N et al (2019) Drug-induced hypertension caused by multikinase inhibitors (Sorafenib, Sunitinib, Lenvatinib and Axitinib) in renal cell carcinoma treatment. Int J Mol Sci 20(19)
14. Decaens T et al (2021) Phase 1b/2 trial of tepotinib in sorafenib pretreated advanced hepatocellular carcinoma with MET overexpression. Br J Cancer 125(2):190–199
15. Hainsworth JD et al (2010) Concurrent radiotherapy and temozolomide followed by temozolomide and sorafenib in the first-line treatment of patients with glioblastoma multiforme. Cancer 116(15):3663–3669
16. Hosseinzadeh F et al (2018) Combinational immune-cell therapy of natural killer cells and sorafenib for advanced hepatocellular carcinoma: a review. Cancer Cell Int 18:133
17. Dattachoudhury S et al (2020) Sorafenib inhibits proliferation, migration and invasion of breast cancer cells. Oncology 98(7):478–486
18. Iyer R et al (2010) Sorafenib: a clinical and pharmacologic review. Expert Opin Pharmacother 11(11):1943–1955
19. Keating GM (2017) Sorafenib: a review in hepatocellular carcinoma. Target Oncol 12(2):243–253
20. Germann UA et al (2017) Targeting the MAPK signaling pathway in cancer: promising preclinical activity with the novel selective ERK1/2 inhibitor BVD-523 (Ulixertinib). Mol Cancer Ther 16(11):2351–2363
21. Ji N et al (2018) Ulixertinib (BVD-523) antagonizes ABCB1- and ABCG2-mediated chemotherapeutic drug resistance. Biochem Pharmacol 158:274–285
22. Buchbinder EI et al (2020) A phase II study of ERK inhibition by ulixertinib (BVD-523) in metastatic uveal melanoma. American Society of Clinical Oncology

23. Jiang H et al (2018) Concurrent HER or PI3K inhibition potentiates the antitumor effect of the ERK inhibitor ulixertinib in preclinical pancreatic cancer models ERK inhibition in pancreatic cancer. 17(10):2144–2155
24. Sullivan RJ et al (2018) First-in-Class ERK1/2 inhibitor ulixertinib (BVD-523) in ;atients with MAPK mutant advanced solid tumors: results of a phase I dose-escalation and expansion study. Cancer Discov 8(2):184–195
25. Tatake RJ et al (2008) Identification of pharmacological inhibitors of the MEK5/ERK5 pathway. Biochem Biophys Res Commun 377(1):120–125
26. Razumovskaya E, Sun J, Rönnstrand L (2011) Inhibition of MEK5 by BIX02188 induces apoptosis in cells expressing the oncogenic mutant FLT3-ITD. Biochem Biophys Res Commun 412(2):307–312
27. Sharma R et al (2022) BMP4 enhances anoikis resistance and chemoresistance of breast cancer cells through canonical BMP signaling. J Cell Commun Signal 16(2):191–205
28. Somaiah C et al (2015) Collagen promotes higher adhesion, survival and proliferation of mesenchymal stem cells. PLoS ONE 10(12):e0145068
29. Carra E et al (2013) Sorafenib selectively depletes human glioblastoma tumor-initiating cells from primary cultures. Cell Cycle 12(3):491–500
30. Yang F et al (2010) Sorafenib induces growth arrest and apoptosis of human glioblastoma cells through the dephosphorylation of signal transducers and activators of transcription 3. Mol Cancer Ther 9(4):953–962
31. Altevogt P et al (2021) Novel insights into the function of CD24: a driving force in cancer. Int J Cancer 148(3):546–559
32. Barash U et al (2019) Heparanase promotes glioma progression via enhancing CD24 expression. Int J Cancer 145(6):1596–1608
33. Ni YH, Zhao X, Wang W (2020) CD24, A review of its role in tumor diagnosis, progression and therapy. Curr Gene Ther 20(2):109–126
34. Wu H et al (2021) Prospects of antibodies targeting CD47 or CD24 in the treatment of glioblastoma. CNS Neurosci Ther 27(10):1105–1117
35. Liu L et al (2006) Sorafenib blocks the RAF/MEK/ERK pathway, inhibits tumor angiogenesis, and induces tumor cell apoptosis in hepatocellular carcinoma model PLC/PRF/5. Cancer Res 66(24):11851–11858
36. Caraglia M et al (2011) Oxidative stress and ERK1/2 phosphorylation as predictors of outcome in hepatocellular carcinoma patients treated with sorafenib plus octreotide LAR. Cell Death Dis 2(4):e150
37. Hsu FT et al (2019) Amentoflavone effectively blocked the tumor progression of glioblastoma via suppression of ERK/NF- κ B signaling pathway. Am J Chin Med 47(4):913–931
38. Hsu FT, Chiang IT, Wang WS (2020) Induction of apoptosis through extrinsic/intrinsic pathways and suppression of ERK/NF-κB signalling participate in anti-glioblastoma of imipramine. J Cell Mol Med 24(7):3982–4000
39. Lopez-Gines C et al (2008) The activation of ERK1/2 MAP kinases in glioblastoma pathobiology and its relationship with EGFR amplification. Neuropathology 28(5):507–515
40. Yu F et al (2021) Wnt/β-catenin signaling in cancers and targeted therapies. Signal Transduct Target Ther 6(1):307
41. Zhang Y, Wang X (2020) Targeting the Wnt/β-catenin signaling pathway in cancer. J Hematol Oncol 13(1):165